Electronic Supplementary Material (ESI) for Reaction Chemistry & Engineering.

Supporting Information

NO reduction with CO over HY Zeolite-Supported Rhodium Dicarbonyl Complexes: giving insight into the structure sensitivity

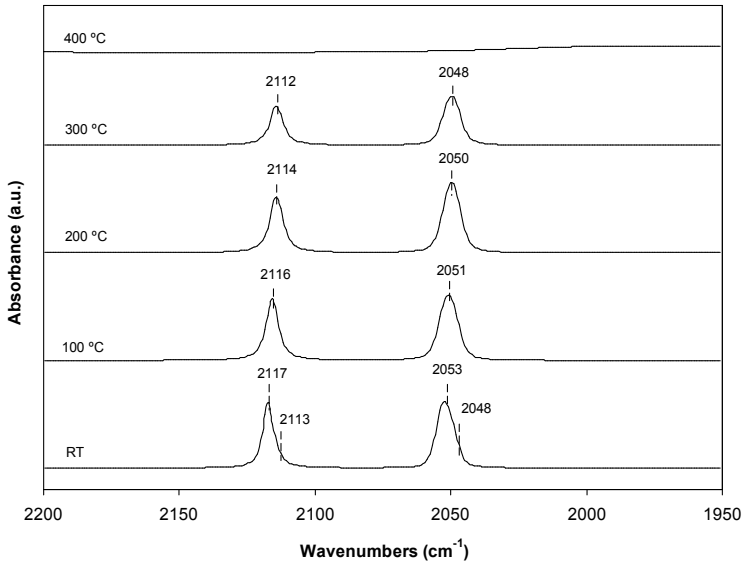

Fig. S1 FTIR spectra in the ν_{CO} region of $Rh(CO)_2$/HY30 sample after treatment in He for 1 h at different temperatures.

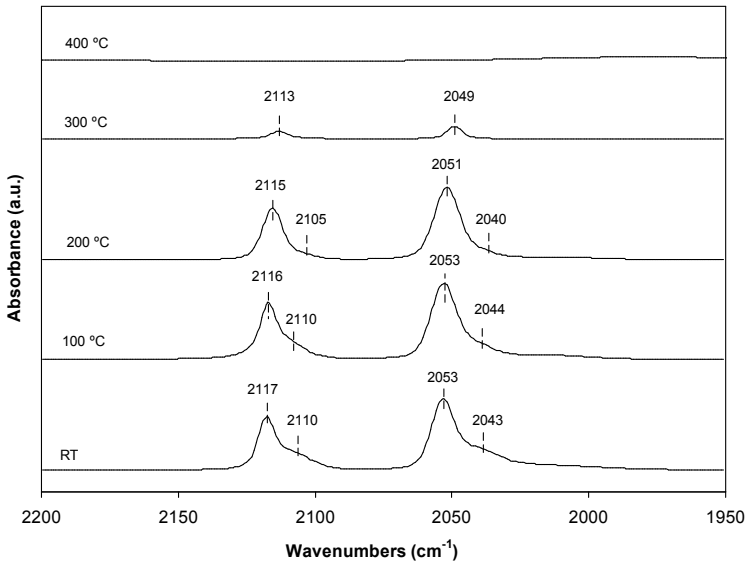

Fig. S2 FTIR spectra in the ν_{CO} region of $Rh(CO)_2$/HY2.6 sample after treatment in He for 1 h at different temperatures.

Table S1. EXAFS structural parameters characterizing $Rh(CO)_2$/HY30 catalyst treated in He for 1 h at different temperatures.

Support	Shell	*N*	*R* (Å)	$\Delta\sigma^2$ (Å^2)	ΔE_0 (eV)	ε_v^2	k^1-variances (%)	
							Im.	Abs.
100 °C	Rh–Rh	--	--	--	--	3.6	3.4	5
	Rh–C*	2.1	1.83	0.00256	10			
	Rh–O*	2	2.99	0.00164	10			
	$Rh–O_{support}$							
	$Rh–O_s$	2.4	2.14	0.00299	-1.8			
	$Rh–O_l$	2.1	2.77	-0.0055	-7.3			
200 °C	Rh–Rh	--	--	--	--	3.4	2.4	3.5
	Rh–C*	2.1	1.83	0.00382	10			
	Rh–O*	1.9	2.97	0.00052	10			
	$Rh–O_{support}$							
	$Rh–O_s$	2.3	2.13	0.00122	-0.6			
	$Rh–O_l$	2.1	2.76	-0.00568	-9.1			
300 °C	Rh–Rh	--	--	--	--	4.4	1.9	2.9
	Rh–C*	0.5	1.82	-0.00318	10			
	Rh–O*	0.6	3.02	-0.00073	0.72			
	$Rh–O_{support}$							
	$Rh–O_s$	1.8	2.17	-0.00173	-5.2			
	$Rh–O_l$	2.4	2.79	-0.00396	-10			
400 °C	Rh–Rh	5.3	2.65	0.00752	7.7	3.1	2	4.2

Standard deviations in fits: *N* ± 20%, *R* ± 1%, $\Delta\sigma^2$ ± 10%, ΔE_0 ± 10%. *N*, coordination number; *R*, distance between absorber and backscatterer atoms; $\Delta\sigma^2$, Debye-Waller factor relative to the Debye-Waller factor of the reference compound; ΔE_0, inner potential correction accounting for the difference in the inner potential between the sample and the reference compound; ε_v^2, goodness of fit; the superscript * refers to carbonyl ligands; *R*-space fit ranges 3.5< k < 15.0 Å^{-1} and 0.5< r < 3.5 Å; 23 allowed fitting parameters.

Table S2. EXAFS structural parameters characterizing $Rh(CO)_2$/HY2.6 catalyst treated in He for 1 h at different temperatures.

Support	Shell	*N*	*R* (Å)	$\Delta\sigma^2$ (Å^2)	ΔE_0 (eV)	ε_v^2	k^1-variances (%)	
							Im.	Abs.
100 °C	Rh–Rh	--	--	--	--	8	2.1	3.1
	Rh–C*	1.9	1.84	0.0015	10.0			
	Rh–O*	2.2	3.00	0.00261	10.0			
	$Rh–O_{support}$							
	$Rh–O_s$	2.1	2.16	0.00192	-3.0			
	$Rh–O_l$	2.4	2.80	-0.00384	-10.0			
200 °C	Rh–Rh	--	--	--	--	7.1	1.8	2.6
	Rh–C*	1.8	1.84	0.00335	10.0			
	Rh–O*	2.2	2.99	0.00397	9.2			
	$Rh–O_{support}$							
	$Rh–O_s$	2.1	2.16	0.00142	-3.1			
	$Rh–O_l$	2.3	2.81	-0.00262	-10.0			
300 °C	Rh–Rh	5.1	2.68	0.00207	5.1	5.2	13.4	30.3
400 °C	Rh–Rh	8.8	2.68	0.00273	6.4	5.4	6.6	9.6

Standard deviations in fits: *N* ± 20%, *R* ± 1%, $\Delta\sigma^2$ ± 10%, ΔE_0 ± 10%. *N*, coordination number; *R*, distance between absorber and backscatterer atoms; $\Delta\sigma^2$, Debye-Waller factor relative to the Debye-Waller factor of the reference compound; ΔE_0, inner potential correction accounting for the difference in the inner potential between the sample and the reference compound; ε_v^2, goodness of fit; the superscript * refers to carbonyl ligands; *R*-space fit ranges 3.5< k < 15.0 Å^{-1} and 0.5< r < 3.5 Å; 23 allowed fitting parameters.

Table S3. EXAFS structural parameters characterizing $Rh(CO)_2$/HY30 (A) and $Rh(CO)_2$/HY2.6 (B) samples before reactants were introduced into the cell at 270 °C.

(A)

Temperature	Shell	*N*	*R* (Å)	$\Delta\sigma^2$ (Å^2)	ΔE_0 (eV)	ε_v^2	k^1-variances (%)	
							Im.	Abs.
270 °C	Rh–Rh	--	--	--	--	2.7	2.4	3.5
	Rh–C*	1.9	1.84	0.00312	10			
	Rh–O*	1.7	2.97	0.00042	9.5			
	$Rh–O_{support}$							
	$Rh–O_s$	2.2	2.13	0.00029	-0.4			
	$Rh–O_l$	2.1	2.76	-0.00505	-8.9			

(B)

Temperature	Shell	*N*	*R* (Å)	$\Delta\sigma^2$ (Å^2)	ΔE_0 (eV)	ε_v^2	k^1-variances (%)	
							Im.	Abs.
270 °C	Rh–Rh	--	--	--	--	10.6	3.3	4.9
	Rh–C*	1.6	1.83	0.00087	6.9			
	Rh–O*	1.5	2.97	0.004	7.6			
	$Rh–O_{support}$							
	$Rh–O_s$	2.1	2.16	0.00157	-6.9			
	$Rh–O_l$	2.2	2.79	-0.00246	-10			

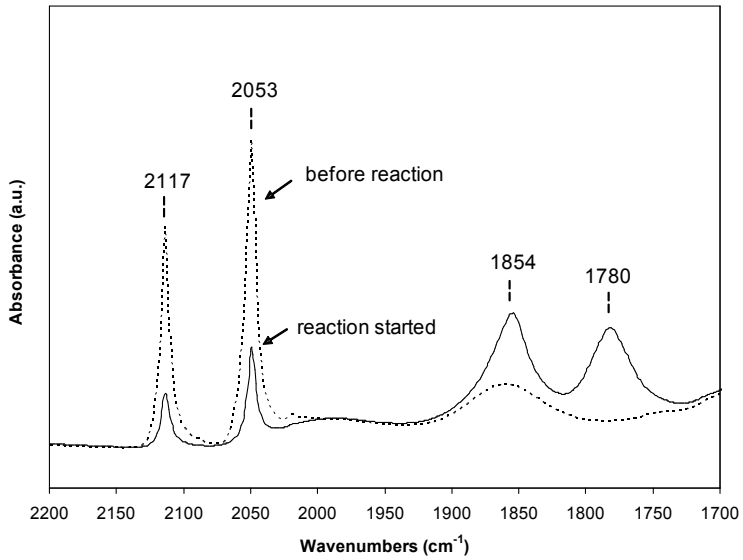

Fig. S3 FTIR spectra in the ν_{CO} and ν_{NO} regions of $Rh(CO)_2$/HY30 sample in He (before reaction) and when 1000 ppm NO 1000 ppm CO was introduced into the cell (reaction started) at 270 °C.

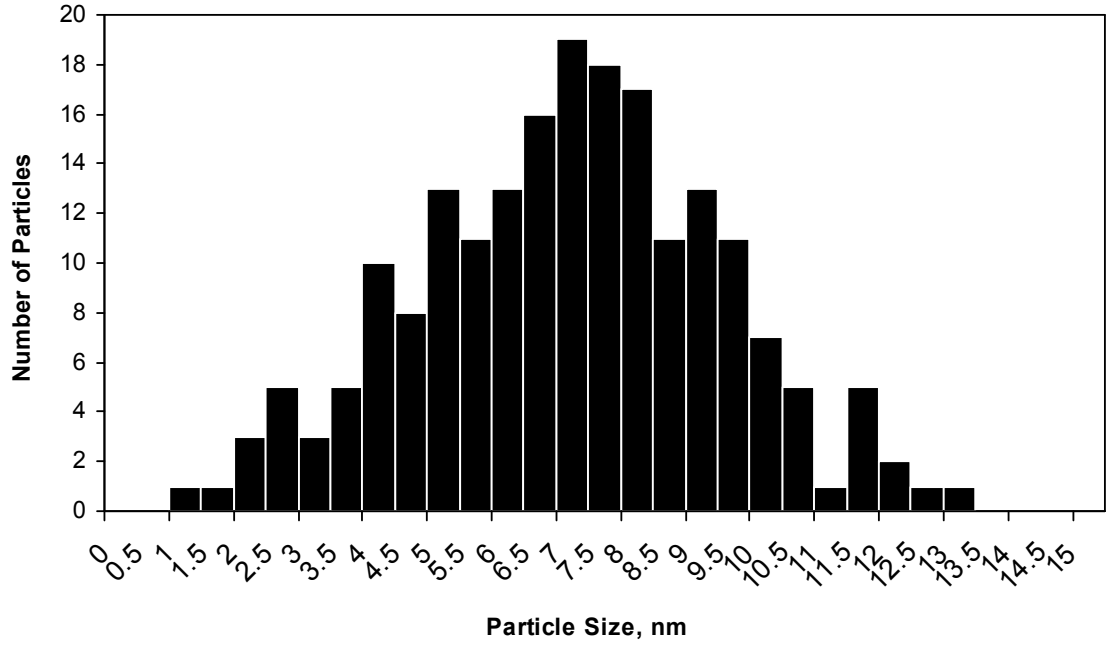

Fig. S4 Particle size distribution histogram (175 particles counted) obtained from HRTEM measurements of used $Rh(CO)_2$/HY2.6 sample (after reaction in 1000 ppm NO, 1000 ppm CO at 270 °C for 200 min).

Table S4. XPS data characterizing $Rh(CO)_2$/HY2.6 sample before (fresh) and after (used) in CO/NO reaction (1000 ppm NO, 1000 ppm CO at 270 °C for 200 min).

Sample	Rh $3d_{5/2}$, eV	FWHM, eV	Rh $3d_{3/2}$, eV	FWHM, eV
fresh	308.5	2.7	313.2	2.7
used	308.6	2.3	313.3	2.3
	307	1.4	311.7	1.4

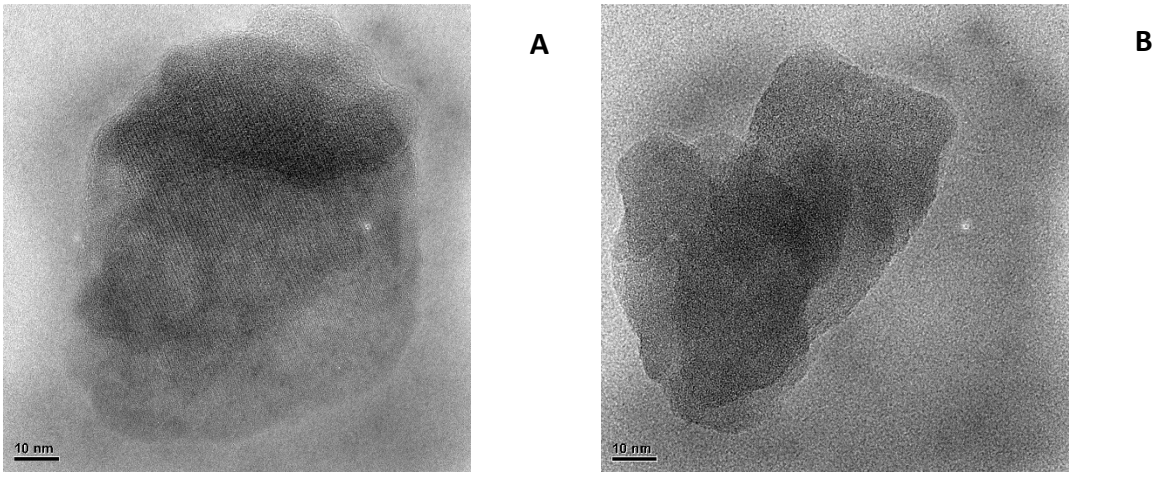

Fig. S5 HRTEM images of $Rh(CO)_2$/HY30 (A) and $Rh(CO)_2$/HY2.6 (B) samples at ambient conditions (initial state of materials before reaction in 1000 ppm NO, 1000 ppm CO at 270 °C).